THE JOURNAL OF PHYSICAL CHEMISTRY B LETTERS

2006, *110,* 4538−4541
Published on Web 02/23/2006

Lithium Environment in Dilute Poly(ethylene oxide)/Lithium Triflate Polymer Electrolyte from REDOR NMR Spectroscopy

Jason R. Wickham,[†] Shawna S. York,[‡] Nathalie M. Rocher,[†] and Charles V. Rice*[,†]

Department of Chemistry and Biochemistry, University of Oklahoma, 620 Parrington Oval, Room 208, Norman, Oklahoma 73019, and Department of Chemistry, Oklahoma Baptist University, Box 61772, Shawnee, Oklahoma 74804.

Received: January 30, 2006

The role of the lithium ion environment is of fundamental interest regarding transport and conductivity in lithium polymer electrolytes. X-ray crystallography has been used to characterize the lithium environment in completely crystalline poly(ethylene oxide) (PEO) electrolytes, but this approach cannot be used with dilute PEO electrolytes. Here, using solid-state NMR data collected with the rotational-echo double-resonance $^{13}C\{^{7}Li\}$ (REDOR) pulse sequence, we have been able to characterize the crystalline microdomains of a PEO−lithium triflate sample with an oxygen/lithium ratio of 20:1. Our data clearly demonstrates that the lithium crystalline microdomains are nearly identical to those of a completely crystalline 3:1 sample, for which the crystal structure is known.

Introduction

Rechargeable lithium ion batteries provide a convenient, portable source of electricity.[1−3] The successful commercialization of this technology resulted from the discovery and development of novel cathode and anode intercalation materials. The electrodes are separated by an inert porous polymer separator, usually poly(propylene), impregnated with low molecular weight organic liquids containing a dissolved salt. However, these organic liquids present a potential fire hazard and may react with the electrode materials. Major efforts to develop solvent-free ion-conducting polymer electrolytes have been underway for 30 years.[2−9] Critical to these efforts is the need to identify the chemical interactions that hinder or facilitate ion transport.

Many laboratories have investigated solid-polymer electrolytes based on poly(ethylene oxide) (PEO), due to its low glass transition temperature (T_g) and its ability to dissolve metal salts.[10−13] Lithium provides a high energy density, yet the room-temperature conductivities of PEO/Li salt systems are too low to replace current liquid or hybrid batteries. Developing a solid polymer electrolyte capable of replacing current electrolytes requires knowledge of lithium transport between the electrodes. Lithium cations are coordinated to the polymer electrolyte through weak chemical interactions. Since these polymer electrolytes have T_g's that are well below room temperature, they have a fair amount of segmental motion. Thus, a lithium cation that is five coordinate will eventually be forced into a four-coordinate conformation due to the segmental motion of the polymer electrolyte. This four-coordinate conformation is less stable than the five-coordinate one, which causes the lithium cation to hop to a neighboring binding site, facilitating lithium transport.[14] For PEO/Li salt systems, impedance measurements can be used to evaluate ion transport,[15] but these measurements do not provide fundamental chemical insight as to the PEO−lithium chemical structure. Low temperature X-ray crystallography data of completely crystalline PEO electrolytes revealed a PEO helix around a central core of lithium cations.[16] Triflate anions, $CF_3SO_3^-$, participate in lithium coordination by forming bridges between two lithium cations.

Dilute PEO electrolytes are heterogeneous at room temperature, consisting of a pure PEO phase, a crystalline PEO−salt phase, and an amorphous phase containing some dissolved salt.[7,13,17−19] It has been observed in numerous PEO−salt systems that ionic conductivity occurs mainly in the amorphous phase.[13] Heating the polymer near 100 °C significantly increases conductivity, which is attributed to a melting of the crystalline phase.[12] There have been various efforts made to reduce the amount of the crystalline phase at room temperature, thereby increasing conductivity, using plasticizers, copolymers, and fillers.[4,20−25] These efforts would benefit from the ability to characterize the lithium environment in dilute polymer electrolytes.

X-ray crystallography cannot be employed to study dilute polymer electrolytes because the samples are heterogeneous and do not possess the long-range structural order necessary for diffraction. However, solid-state NMR is ideally suited to provide structural data for the various domains within dilute polymer electrolytes. Previous solid-state NMR studies of PEO or PEO-based polymer electrolytes have examined the connection between ion diffusion and polymer segmental motion. Spin−lattice relaxation and pulse field gradient measurements of ^{7}Li and ^{19}F yield ion diffusion rates, which are used to gauge the success of polymer electrolyte modifications.[26−34] The ^{7}Li spectrum can also be used to identify the number of lithium binding sites.[35,36] Carbon-13 magic angle spinning (MAS) NMR

* Corresponding author. E-mail: rice@ou.edu.
† University of Oklahoma.
‡ Oklahoma Baptist University.

10.1021/jp060643m CCC: $33.50

experiments have been used to detect the amorphous and crystalline regions of PEO electrolytes,[37−40] study polymer dynamics with T_1 experiments,[30,39,41,42] detect backbone inorganic filler interactions,[43] and measure the distance between the backbone CH_2's and the triflate CF_3.[44] Static ^{13}C solid-state experiments have been used to study polymer−cation interactions.[45,46] Nonetheless, these solid-state NMR experiments cannot provide the detailed structural information available from rotational-echo double-resonance (REDOR) data. This has been demonstrated by the recent REDOR study of a crystalline 6:1 PEO/$LiPF_6$ sample,[47] which agreed with the previously published X-ray structure.

In this paper we use the $^{13}C\{^7Li\}$ REDOR pulse sequence to study the PEO−lithium triflate (PEO/LiTf) solid polymer electrolyte system. Dilute PEO/LiTf systems are composed of amorphous and crystalline regions that contain lithium triflate. Although many ion conductivity mechanisms are based on transport through the amorphous region, it is difficult to collect NMR data for the amorphous phase alone because the two NMR signals overlap.[47] However, the rotating-frame spin−lattice relaxation rate ($T_1\rho$) for the amorphous signal is much faster than that for the crystalline phase. By collecting REDOR data after a long cross-polarization time, the NMR signal is due solely to the crystalline region. Understanding the structure of the crystalline microdomains is vital in developing methods to liberate the lithium cations trapped within them. $^{13}C\{^7Li\}$ REDOR NMR data was collected for the completely crystalline 3:1 PEO/LiTf and the crystalline microdomains for the 20:1 PEO/LiTf. Our data clearly demonstrates that the lithium crystalline microdomains are nearly identical to those of a completely crystalline 3:1 sample, for which the crystal structure is known. Similar structural investigations of the amorphous regions are of great interest, and efforts to analyze these data, collected in the presence of the crystalline NMR signal, are underway.

Experimental Section

Sample Preparation. PEO, with an average molecular weight of 2000, was obtained from Polysciences, Inc. and was used as received. Anhydrous acetonitrile (99.8%) was obtained from Aldrich and used as received. Lithium trifluoromethanesulfonate (lithium triflate, LiTf) was obtained from Aldrich and dried in a vacuum oven at 120 °C for 48 h prior to use. All chemicals were stored and used in a dry argon atmosphere glovebox with moisture less than 1 ppm. Polymer−salt solutions were prepared by dissolving weighed amounts of PEO and LiTf in dry acetonitrile and stirring for 24 h to ensure a homogeneous solution. To obtain the polymer electrolyte sample, the solutions were cast onto Teflon sheets, and the acetonitrile was allowed to evaporate in the glovebox for 48 h. After the NMR data was collected, the absence of water in the samples was confirmed by Fourier transform infrared (FT-IR) measurements made with a Bruker IFS-66V FT-IR, recorded over the range of 400−4000 cm^{-1} at a resolution of 1 cm^{-1}.

NMR Experiments. All solid-state experiments were performed using a three-channel Varian UnityInova NMR spectrometer ($B_o = 7$ T) with a 5 mm, three-channel, MAS Varian APEX probe. NMR samples were packed into zirconia pencil rotors inside a dry glovebox. A boron nitride spacer and plug were used and sealed with epoxy to prevent contamination by atmospheric moisture. Drive and bearing gas were provided by dry, compressed air. The ^{13}C chemical shifts were referenced to an external standard of glycine (carbonyl resonance at 176.4 ppm). The sample temperature was maintained at 25 °C throughout the NMR data collection. Data acquisition and processing was accomplished with VNMRJ (version 1.1D) provided by Varian Inc.

REDOR data were collected using a sample spinning rate of 5000 Hz, a cross-polarization contact time of 8000 μs, and ^1H decoupling at a radio frequency (rf) power level of 50 kHz. The rf powers for the ^{13}C and ^7Li channels were 50 and 86 kHz, respectively. The XY-8 phase cycling scheme was used on both the ^{13}C and ^7Li channels.[48] S_o and S_r spectra were recorded at 2, 4, 6, 8, ..., 40 rotor cycles. Each spectrum was collected with 256 scans and a 20 s recycle time (^1H $T_1 = 7$ s). Each $^{13}C\{^7Li\}$ REDOR data point was divided by 0.93 to scale for the natural abundance of ^7Li.

REDOR is used in solid-state NMR to measure dipole−dipole coupling between heteronuclei.[49,50] Detailed mathematical and pictorial descriptions of REDOR have been reported.[48−51] The REDOR experiment requires the acquisition of 2 NMR spectra collected under MAS conditions. The first spectrum, labeled S_0, is collected using decoupling (^1H) and observe spin (denoted S-spin, ^{13}C) rf pulses only. Between the pulses and data acquisition, dipolar-coupling effects are averaged away by the use of MAS, and the signals have full intensity. A second spectrum, labeled S_r, is collected using identical ^1H and ^{13}C pulses, with rf pulses applied to another nucleus (denoted the I-spin, ^7Li for these experiments) at selected intervals. The I-spin pulses reintroduce the dipolar interaction that otherwise would be averaged away by MAS.

The dipole−dipole interaction causes a transverse dephasing of the magnetization, reducing the signal intensity. Subtracting the "dephased-echo" spectrum (S_r) from the full-echo (S_0) spectrum provides a difference spectrum (ΔS). Although the I-spin rf pulses that cause dephasing each have a fixed duration, the amount of transverse dephasing can be increased by using more pulses. Longer dephasing times decrease S_r, increasing ΔS. The distance between ^{13}C and ^7Li can be found by relating the intensity of ΔS to the dephasing time. However, other T_2 processes may cause additional signal loss, affecting both S_0 and S_r, so their effect is corrected for by dividing ΔS by S_0.

A plot of $\Delta S/S_o$ versus dephasing time yields the REDOR dephasing curve. The SIMPSON program[52] calculates a theoretical dephasing curve based on the nuclear spin system and the dipolar-coupling constants. The distance between the interacting spins can be extracted from the strength of the dipole−dipole coupling using eq 1:

$$D = (\mu_o h/4\pi)(\gamma^I \gamma^S/r^3) \quad (1)$$

where D is the dipolar-coupling constant, μ_o is the permittivity of free space, γ^I is the magnetogyric ratio of the dephasing nuclei (^7Li), γ^S is the magnetogyric ratio of the observe nuclei (^{13}C), and r is the internuclear distance.

Fitting Procedure. From the reported PEO_3/LiTf crystal structure,[16] the distance from any carbon to the closest (primary) lithium varies from 2.55 to 3.40 Å. However, the second and third closest (secondary and tertiary) lithium atoms are close enough for weak dipolar interactions with the carbon atoms. Thus, a ^{13}C nucleus may be dephased by several ^7Li nuclei at different distances. However, at short dephasing times (0−2.5 ms), ^{13}C signal loss is caused by the primary lithium due to its much larger dipolar coupling, whereas the secondary and tertiary lithium atoms do not have a significant effect until dephasing times of 3−8 ms.

Dipolar-coupling constants were determined from SIMPSON[52] simulation that generate a theoretical REDOR dephasing curve. Simulations involving one ^{13}C and one ^7Li were compared

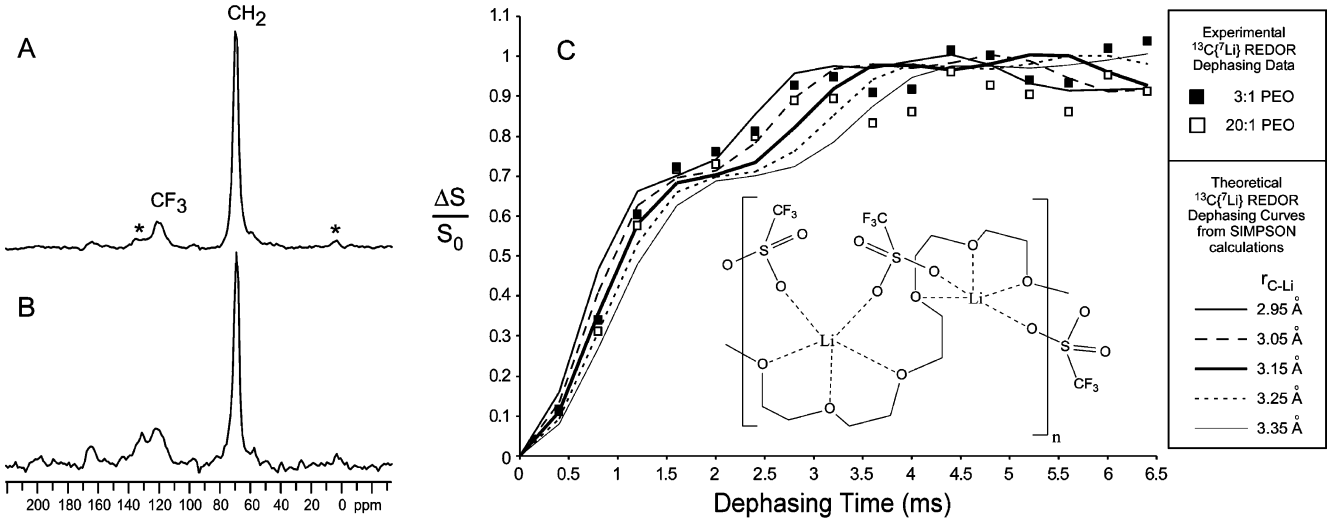

Figure 1. (A) ^{13}C CP-MAS of 2000 MW PEO lithium triflate: O/Li = 3:1; (B) ^{13}C CP-MAS of 2000 MW PEO lithium triflate: O/Li = 20:1. B_0 = 7 T, contact time = 8 ms, spinning rate = 5 kHz, recycle time = 20 s, line broadening = 100 Hz, line width = 330 Hz, and scans = 256 for A and B. (C) ^{13}C{^{7}Li} REDOR dephasing curve for 3:1 PEO/LiTf and 20:1 PEO/LiTf signals.

to the first four data points to determine the primary lithium−carbon dipolar-coupling constant. From this dipolar-coupling constant, the average primary Li−C distances were calculated using eq 1. Multiple spin simulations are necessary to model the data past 3 ms and were found to be computationally difficult.

Results and Discussion

Figure 1A,B shows the ^{13}C CPMAS spectra for 3:1 and 20:1 PEO/LiTf. As expected, single peaks are seen for the polymer backbone (CH_2) and the triflate (CF_3) groups. These spectra were taken under the same experimental parameters; however, the 20:1 sample has a much lower signal-to-noise ratio. This arises because only a small fraction of the sample is solid on the NMR time scale. Solid-state NMR uses cross-polarization to selectively observe the solid fraction.[38−40,53] Because the cross-polarization dynamics in the 20:1 sample is similar to that in the highly crystalline 3:1 sample, the signal in Figure 1B is assigned to the microcrystalline domains within the heterogeneous 20:1 polymer electrolyte sample. Efforts to quantify the microcrystalline fraction are underway and do not affect the ability of REDOR to characterize the lithium environment.

REDOR dephasing curves for 3:1 and 20:1 PEO/LiTf are shown in Figure 1C. These data points do not have the typical shape of the universal REDOR curve, which describes the dipolar coupling between two spin 1/2 nuclei. Our data originated from the dipolar coupling between spin 1/2 (^{13}C) and spin 3/2 (^{7}Li) nuclei, and the SIMPSON program was used to simulate the REDOR dephasing curve. Our REDOR data have the correct shape and intensity that is expected from the full excitation of the ^{7}Li spins, based on the results of our SIMPSON simulations and by comparison with the work by Reichert et al.[47]

From the SIMPSON results and our REDOR dephasing data, the distance between the CH_2 and the primary (closest) lithium is 3.15 ± 0.1 Å. This value is 6% longer than the average Li−C distance from the PEO_3/LiTf crystal structure (2.975 Å) published by Lightfoot et al.,[16] which is expected for distances obtained from REDOR. It is well established that distances obtained from REDOR measurements are longer than those obtained from X-ray diffraction[54−56] due to the effects of vibrational and librational motion on the dipolar interaction.[55]

Distances to the secondary and tertiary lithium atoms are 6−7 Å, according to the crystal structure. These dipolar couplings, although weak, result in a deviation of the simulations from the experimental data. Three-spin and four-spin SIMPSON simulations are computationally intensive, given the need to fit several distances and numerous dihedral angles. Fortunately, we can describe the microcrystal architecture through comparison with data collected for a completely crystalline sample, 3:1 PEO/LiTf.

The REDOR dephasing data for PEO/LiTf (20:1) are essentially identical to the 3:1 data in the region of 0−2.5 ms. Beyond 3 ms, the 20:1 data points are slightly lower than the 3:1 data points, yet they retain the same sinusoidal shape. The REDOR dephasing curve arises from the dipolar interaction with the lithium cation. However, dilute PEO/LiTf systems, such as the 20:1 system, have a small amount of crystalline PEO that does not contain lithium triflate. These crystalline, lithium free, PEO segments contribute to the S_o signal, but not to the S_r signal. SIMPSON simulations, and the 3:1 data points, show that the plot of $\Delta S/S_0$ should reach unity, whereas the 20:1 data rise to a value of 0.95. Thus, we can estimate that 5% of the crystalline segments are not dephased by secondary or tertiary lithium atoms. These PEO segments are affected by a primary lithium cation because the 20:1 data closely follow the 3:1 data from 0 to 2.5 ms. Such a chemical environment could arise at the edges of the crystalline microdomains. Strikingly, the initial slope of the dephasing curves for PEO/LiTf 3:1 and 20:1 indicates that the average primary Li−C distances must be very similar. Together with the similar sinusoidal nature from 2.5 to 8 ms, these data suggest that the 20:1 and 3:1 compounds have nearly identical local structures inside their respective crystalline fractions. Thus, the molecular architecture within the microcrystalline domain of 20:1 is almost certainly a helix, the known structure of the 3:1 compound.

Conclusions

REDOR is a valuable tool for measuring molecular structures of nonrefractive materials, including solid polymer electrolytes. It has been demonstrated by Rhodes and Frech that X-ray data for 20:1 PEO/LiTf contain no diffraction peaks for the crystalline region.[12,57] We show that it is not only possible to observe the crystalline region of a 20:1 sample with solid-state NMR, but

REDOR data also give structural information for the microcrystalline domain. The lithium environment in the microcrystalline domains of PEO/LiTf 20:1 is indistinguishable from the much larger crystal regions of PEO_3/LiTf, for which a crystal structure is known.

The presence of a crystalline region in 20:1 PEO/LiTf is consistent with published phase diagrams[19] and information that has been inferred from vibrational spectroscopy studies.[57] To the best of our knowledge, this is the first direct structural measurement for the crystalline region of a dilute polymer electrolyte−lithium salt system. Using REDOR to understand the microscopic structure of solid polymer electrolytes is a first step toward future improvements in both conductivity and material properties. Such structural information identifies the molecular interactions that retard lithium ion mobility, providing chemical targets to increase conductivity. Likewise, REDOR will prove to be a powerful tool to evaluate molecular-level engineering strategies aimed toward alleviating crystalline domains.

Acknowledgment. This work is supported by the American Chemical Society Petroleum Research Fund (41463-G10) and by the National Science Foundation (EPS-0132534). S.S.Y. thanks the American Chemical Society Petroleum Research Fund for a Summer Research Fellowship. We thank Jerry Chan and the SIMPSON/SIMMOL Discussion Boards for help with SIMPSON input files, and Roger Frech for the use of his glovebox and FT-IR spectrometer.

References and Notes

(1) Dresselhaus, M. S.; Thomas, I. L. *Nature* **2001**, *414* (6861), 332−337.
(2) Tarascon, J.-M.; Armand, M. *Nature* **2001**, *414*, 359−367.
(3) Sadoway, D. R.; Mayes, A. M. *MRS Bull.* **2002**, *27* (8), 590−592.
(4) Croce, F.; Appetecchi, G. B.; Persi, L.; Scrosati, B. *Nature* **1998**, *394* (6692), 456−458.
(5) Armand, M. *Solid State Ionics* **1983**, *9*−*10*, 745−754.
(6) Gauthier, M.; Bélanger, A.; Kapfer, B.; Vassort, G.; Armand, M. Solid Polymer Electrolyte Lithium Batteries. In *Polymer Electrolyte Reviews*; Vincent, C. A., Ed.; Elsevier: London, 1989; Vol. 2, pp 285−332.
(7) Gadjourova, Z.; Andreev, Y. G.; Tunstall, D. P.; Bruce, P. G. *Nature* **2001**, *412* (6846), 520−523.
(8) Andreev, Y. G.; Bruce, P. G. *J. Phys.: Condens. Matter* **2001**, *13* (36), 8245−8255.
(9) Wright, P. V. *Br. Polym. J.* **1975**, *7*, 319−327.
(10) Papke, B. L.; Ratner, M. A.; Shriver, D. F. *J. Electrochem. Soc.* **1982**, *129* (7), 1434−1438.
(11) Frech, R.; Chintapalli, S.; Bruce, P. G.; Vincent, C. A. *Chem. Commun.* **1997**, *2*, 157−158.
(12) Frech, R.; Chintapalli, S.; Bruce, P. G.; Vincent, C. A. *Macromolecules* **1999**, *32* (3), 808−813.
(13) Berthier, C.; Gorecki, W.; Minier, M.; Armand, M. B.; Chabagno, J. M.; Rigaud, P. *Solid State Ionics* **1983**, *11* (1), 91−95.
(14) Ratner, M. A.; Shriver, D. F. *Chem. Rev.* **1988**, *88* (1), 109−124.
(15) Bruce, P. G. C., Stephen, A.; Lightfoot, P.; Mehta, M. A. *Solid State Ionics* **1995**, *78* (3,4), 191−198.
(16) Lightfoot, P.; Mehta, M. A.; Bruce, P. G. *Science* **1993**, *262* (5135), 883−885.
(17) Fauteux, D.; McCabe, P. *Polym. Adv. Technol.* **1995**, *6* (2), 83−90.
(18) Lascaud, S.; Perrier, M.; Vallee, A.; Besner, S.; Prud′homme, J.; Armand, M. *Macromolecules* **1994**, *27* (25), 7469−7477.
(19) Vallee, A.; Besner, S.; Prud′homme, J. *Electrochim. Acta* **1992**, *37*, 1579−1583.
(20) Kelly, I.; Owen, J. R.; Steele, B. C. H. *J. Electroanal. Chem. Interfacial Electrochem.* **1984**, *168*, 467−478.
(21) Wang, C.; Liu, Q.; Cao, Q.; Meng, Q.; Yang, L. *Solid State Ionics* **1992**, *53*−*56*, 1106−1110.
(22) Walls, H. J.; Riley, M. W.; Singhal, R. R.; Spontak, R. J.; Fedkiw, P. S.; Khan, S. A. *Adv. Funct. Mater.* **2003**, *13* (9), 710−717.
(23) Yang, D. K.; Zax, D. B. *J. Chem. Phys.* **1999**, *110* (11), 5325−5336.
(24) Bronstein, L. M.; Joo, C.; Karlinsey, R.; Ryder, A.; Zwanziger, J. W. *Chem. Mater.* **2001**, *13* (10), 3678−3684.
(25) Chandrasekhar, V. *Adv. Polym. Sci.* **1998**, *135*, 139−205.
(26) Roux, C.; Gorecki, W.; Sanchez, J.-Y.; Jeannin, M.; Belorizky, E. *J. Phys.: Condens. Matter* **1995**, *7*, 6823−6832.
(27) Roux, C.; Gorecki, W.; Sanchez, J.-Y.; Jeannin, M.; Belorizky, E. *J. Phys.: Condens. Matter* **1996**, *8*, 7005−7017.
(28) Golodnitshy, D.; Livshits, E.; Ulus, A.; Barkay, Z.; Lapides, I.; Peled, E.; Chung, S. H.; Greenbaum, S. *J. Phys. Chem. A* **2001**, *105*, 10098−10106.
(29) Hong, L.; Shi, L.; Tang, X. *Macromolecules* **2003**, *36*, 4989−4994.
(30) Souza, P. H. d.; Bianchi, R. F.; Dahmouche, K.; Judeinstein, P.; Faria, R. M.; Bonagamba, T. J. *Chem. Mater.* **2001**, *13*, 3685−3692.
(31) Adebahr, J.; Best, A. S.; Byrne, N.; Jacobsson, P.; MacFarlane, D. R.; Forsyth, M. *Phys. Chem. Chem. Phys.* **2003**, *5*, 720−725.
(32) Wong, S.; Vasudevan, S.; Vaia, R. A.; Giannelis, E. P.; Zax, D. B. *J. Am. Chem. Soc.* **1995**, *117*, 7568−7569.
(33) Mustarelli, P.; Capiglia, C.; Quartarone, E.; Tomasi, C.; Ferloni, P. *Phys. Rev. B* **1999**, *60*, 7228−7233.
(34) Adamic, K. J.; Greenbaum, S. G.; Abraham, K. M.; Alamgir, M.; Wintersgill, M. C.; Fontanella, J. J. *Chem. Mater.* **1991**, *3*, 534−538.
(35) Liang, W.-J.; Kuo, C.-L.; Lin, C.-L.; Kuo, P.-L. *J. Polym. Sci., Part A: Polym. Chem.* **2002**, *40*, 1226−1235.
(36) Liang, W.-J.; Kuo, P.-L. *Macromolecules* **2004**, *37*, 840−845.
(37) Spevacek, J.; Brus, J.; Dybal, J. *Solid State Ionics* **2004**, *176* (1−2), 163−167.
(38) Jiri Spevacek, J. D. *Macromol. Rapid Commun.* **1999**, *20*, 435−439.
(39) Bartolotta, A. F., Claudia; Geppi, Marco; Minniti, Domenico; Visalli, Giuseppe. *Solid State Nucl. Magn. Reson.* **1997**, *8* (4), 231−239.
(40) Kuo, P.-L.; Hou, S.-S.; Lin, C.-Y.; Chen, C.-C.; Wen, T.-C. *J. Polym. Sci., Part A: Polym. Chem.* **2004**, *42*, 2051−2059.
(41) Mello, N. C.; Bonagamba, T. J.; Panepucci, H.; Dahmouche, K.; Judeinstein, P.; Aegerter, M. A. *Macromolecules* **2000**, *33*, 1280−1288.
(42) Spindler, R.; Shriver, D. F. *J. Am. Chem. Soc.* **1988**, *110*, 3036−3043.
(43) Quartarone, E.; Mustarelli, P.; Tomasi, C.; Magistris, A. *J. Phys. Chem. B* **1998**, *102*, 9610−9616.
(44) Spevacek, J.; Brus, J. *Macromol. Symp.* **2003**, *203*, 111−121.
(45) Arun, N.; Vasudevan, S.; Ramanathan, K. V. *J. Chem. Phys.* **2003**, *119*, 2840−2848.
(46) Giotto, M. V.; Sangiorge, C. L.; Harris, D. J.; de Oliveira, A. L.; Schmidt-Rohr, K.; Bonagamba, T. J. *Macromolecules* **2002**, *35*, 3576−3583.
(47) Reichert, D.; Pascui, O.; Judeinstein, P.; Gullion, T. *Chem. Phys. Lett.* **2005**, *402* (1−3), 43−47.
(48) Gullion, T. *Concepts Magn. Reson.* **1998**, *10* (5), 277−289.
(49) McDowell, L. M.; Schaefer, J. *Curr. Opin. Struct. Biol.* **1996**, *6*, 624−629.
(50) Schaefer, J. REDOR and TEDOR. In *Encyclopedia of Nuclear Magnetic Resonance*, Harris, R. K., Ed.; John Wiley: New York, 1996; pp 3983−3984.
(51) Gullion, T.; Schaefer, J. *J. Magn. Reson.* **1989**, *81*, 196−200.
(52) Bak, M.; Rasmussen, J. T.; Nielsen, N. C. *J. Magn. Reson.* **2000**, *147* (2), 296−330.
(53) Spevacek, J.; Brus, J.; Dybal, J. *Solid State Ionics* **2005**, *176* (1−2), 163−167.
(54) Boman, A.; Edlund, U.; Forster, H.; Johnels, D. *Acta Chem. Scand.* **1999**, *53* (9), 699−702.
(55) Ishii, Y.; Terao, T.; Hayashi, S. *J. Chem. Phys.* **1997**, *107* (8), 2760−2774.
(56) Smith, L. J.; Boulineau, F. P.; Raftery, D.; Wei, A. *J. Am. Chem. Soc.* **2003**, *125* (49), 14958−14959.
(57) Rhodes, C. P.; Frech, R. *Macromolecules* **2001**, *34* (8), 2660−2666.